Electric field induced crossings of energy terms of a Rydberg quasi molecule enhancing charge exchange and ionization

N. Kryukov and E. Oks

Abstract: Charge exchange is one of the most important atomic processes in plasmas. Charge exchange and crossings of corresponding energy levels that enhance charge exchange are strongly connected with problems of energy losses and of diagnostics in high temperature plasmas. Charge exchange was also proposed as an effective mechanism for population inversion in the soft X-ray and vacuum ultraviolet ranges. One of the most fundamental theoretical domains for studying charge exchange is the problem of electron terms in the field of two stationary Coulomb centers (TCC) of charges Z and Z' separated by a distance R. It presents an intriguing atomic physics: the terms can have crossings and quasi crossings. These intrinsic features of the TCC problem also manifest in different areas of physics, such as plasma spectroscopy: a quasi crossing of the TCC terms, by enhancing charge exchange, can result in an unusual structure (a dip) in the spectral line profile emitted by a Z-ion from a plasma consisting of both Z- and Z'-ions, as was shown theoretically and experimentally. Before the year 2000, the paradigm was that the preceding sophisticated features of the TCC problem and its flourishing applications were inherently quantum phenomena. In 2000, a purely classical description of the crossings of energy terms was presented. In the present paper we study the effect of an electric field (along the internuclear axis) on circular Rydberg states of the TCC system. We provide analytical results for strong fields, as well as numerical results for moderate fields. We show that the electric field has several effects. First, it leads to the appearance of an extra energy term: the fourth classical energy term — in addition to the three classical energy terms at zero field. Second, but more importantly, the electric field creates additional crossings of these energy terms. We show that some of these crossings significantly enhance charge exchange, while other crossings enhance the ionization of the Rydberg quasi molecule.

PACS Nos: 32.60.+i, 32.80.Ee, 34.70.+e, 33.80.Be, 31.15.–p

Résumé : L'échange de charge est le plus important mécanisme atomique dans les plasmas. L'échange de charge et le croisement des niveaux d'énergie correspondants qui augmente l'échange de charge sont fortement connectés aux problèmes de perte d'énergie et de diagnostique dans les plasmas de haute température. L'échange de charge a aussi été proposé comme un mécanisme efficace pour l'inversion de population dans les domaines VUV et rayon-X mou. Le problème des termes de l'électron dans le champ de deux centres coulombiens stationnaires (TCC) de charges Z et Z' séparés par une distance R, est central dans l'étude de l'échange de charge. C'est un problème intriguant en physique atomique : les termes peuvent avoir des croisements et des quasi croisements. Ces caractéristiques intrinsèques se manifestent également dans d'autres domaines de la physique, comme la spectroscopie du plasma : un quasi croisement des termes TCC, par augmentation de l'échange de charge, peut donner une structure inhabituelle (un creux) dans le profile de raies spectrales émis par un ion Z dans un plasma contenant des ions Z et Z', comme il a été démontré expérimentalement et théoriquement. Avant l'an 2000, le paradigme était que les caractéristiques sophistiquées du problème TCC et ses applications croissantes étaient des phénomènes essentiellement quantiques. En 2000, est apparue une description purement classique des termes de croisement. Ici, nous étudions l'effet du champ électrique (le long de l'axe internucléaire) sur les états circulaires de Rydberg du système TCC. Nous présentons des résultats analytiques en champ fort, ainsi que des résultats numériques pour champs intermédiaires. Nous montrons que le champ électrique a différents effets. En premier, il mène à l'apparition d'un terme d'énergie additionnel : le quatrième terme d'énergie — en addition aux trois termes classiques d'énergie en champ nul. Deuxièmement, mais plus important, le champ électrique génère des croisements additionnels de ces termes d'énergie. Nous montrons que certains de ces croisements augmente de façon significative l'échange de charge, alors que d'autres croisements augmentent l'ionisation de la quasi molécule de Rydberg.

[Traduit par la Rédaction]

Received 16 February 2012. Accepted 1 May 2012. Published at www.nrcresearchpress.com/cjp on 8 June 2012.

N. Kryukov and E. Oks. Physics Department, 206 Allison Laboratory, Auburn University, Auburn, AL 36849, USA.

Corresponding author: Eugene Oks (e-mail: goks@physics.auburn.edu).

1. Introduction

Charge exchange is one of the most important atomic processes in plasmas. Charge exchange and crossings of corresponding energy levels that enhance charge exchange are strongly connected with problems of energy loss and of diagnostics in high temperature plasmas (see, e.g., refs. 1, 2, and references therein). Charge exchange was proposed as an effective mechanism for population inversion in the soft X-ray and vacuum ultraviolet ranges [3–6]. One of the most fundamental theoretical domains for studying charge exchange is the problem of electron terms in the field of two stationary Coulomb centers (TCC) of charges Z and Z' separated by a distance R. It presents an intriguing atomic physics: the terms can have crossings and quasi crossings.

The crossings are due to the fact that the well-known Neumann–Wigner general theorem on the impossibility of crossing of terms of the same symmetry [7] is not valid for the TCC problem of $Z' \neq Z$ [8]. Physically it is here a consequence of the fact that the TCC problem allows a separation of variables in the elliptic coordinates [8]. As for the quasi crossings, they occur when two wells, corresponding to separated Z- and Z'-centers, have states Ψ and Ψ', characterized by the same energies $E = E'$, by the same magnetic quantum numbers $m = m'$, and by the same radial elliptical quantum numbers $k = k'$ [9–11]. In this situation, the electron has a much larger probability of tunneling from one well to the other (i.e., of charge exchange) as compared to the absence of such degeneracy.

These intrinsic features of the TCC problem also manifest in a different area of physics, such as plasma spectroscopy as explained herein. A quasi crossing of the TCC terms, by enhancing charge exchange, can result in unusual structures (dips) in the spectral line profile emitted by a Z-ion from a plasma consisting of both Z- and Z'-ions, as was shown theoretically and experimentally [12–17].

Before the year 2000, the paradigm was that the preceding sophisticated features of the TCC problem and its flourishing applications were inherently quantum phenomena. But then in 2000 one of the authors published papers [18, 19] presenting a purely classical description of both the crossings of energy levels in the TCC problem and the dips in the corresponding spectral line profiles caused by the crossing (via enhanced charge exchange). These classical results were obtained analytically based on first principles without using any model assumptions. Later, applications of these results included a magnetic stabilization of Rydberg quasi molecules [20] and a problem of continuum lowering in plasmas [21].

In refs. 18, 20, and 21 the study was focused on circular Rydberg states (CRS) of the TCC system (the analysis in ref. 19 went beyond CRS). CRS of atomic and molecular systems with only one electron correspond to $|m| = (n - 1) \gg 1$, where n and m are the principal and magnetic electronic quantum numbers, respectively. They have been extensively studied [22–25] both theoretically and experimentally for several reasons: (*i*) CRS have long radiative lifetimes and highly anisotropic collision cross sections, thereby enabling experiments on inhibited spontaneous emission and cold Rydberg gases [26, 27], (*ii*) classical CRS correspond to quantal coherent states, objects of fundamental importance, and (*iii*) a classical description of CRS is the primary term in the quantal method based on the $1/n$-expansion (see, e.g., ref. 28 and references therein).

While the authors of ref. 20 studied analytically the effect of a magnetic field (along the internuclear axis) on CRS of the TCC system, in the present paper we study the effect of an electric field (along the internuclear axis) on CRS of the TCC system. We provide analytical results for strong fields, as well as numerical results for moderate fields. We show that the electric field leads to the following consequences.

First, it leads to the appearance of an extra energy term: the fourth classical energy term, in addition to the three classical energy terms at zero field. Second, but more importantly, the electric field creates additional crossings of these energy terms. We show that some of these crossings enhance charge exchange while other crossings enhance the ionization of the Rydberg quasi molecule.

The enhancement of charge exchange by the electric field has a practical application to the feasibility of controlled fusion in tokamaks. More details on this are given in the Conclusion.

2. Calculations of the classical Stark effect for a Rydberg quasi molecule in a circular state

We consider a TCC system, where the charge Z is at the origin and the O–z axis is directed to the charge Z', which is at $z = R$ (here and later the atomic units $\hbar = e = m_e = 1$ are used). A uniform electric field $\boldsymbol{F}$ is applied along the internuclear axis in the negative direction of the O–z axis. We study CRS where the electron moves around a circle in the plane perpendicular to the internuclear axis, the circle being centered at this axis.

Two quantities, the energy E and the projection L of the angular momentum on the internuclear axis are conserved in this configuration. We use cylindrical coordinates to write the equations for both.

$$E = \frac{1}{2}\left[\left(\frac{\mathrm{d}\rho}{\mathrm{d}t}\right)^2 + \rho^2\left(\frac{\mathrm{d}\phi}{\mathrm{d}t}\right)^2 + \left(\frac{\mathrm{d}z}{\mathrm{d}t}\right)^2\right] - \frac{Z}{r} - \frac{Z'}{r'} - Fz \qquad (1)$$

$$L = \rho^2\frac{\mathrm{d}\phi}{\mathrm{d}t} \qquad (2)$$

where ρ is the distance of the electron from the internuclear axis, φ is its azimuthal angle, z is the projection of the radius vector of the electron on the internuclear axis, r and r' are the distances of the electron from the particle to Z and Z', respectively.

The circular motion implies that $\mathrm{d}\rho/\mathrm{d}t = 0$; as the motion occurs in the plane perpendicular to the z-axis, $\mathrm{d}z/\mathrm{d}t = 0$. Further, expressing r and r' through ρ and z, and taking $\mathrm{d}\varphi/\mathrm{d}t$ from (2), we have:

$$E = \frac{L^2}{2\rho^2} - \frac{Z}{\left(\rho^2 + z^2\right)^{1/2}} - \frac{Z'}{\left[\rho^2 + (R - z)^2\right]^{1/2}} - Fz \qquad (3)$$

With the scaled quantities

$$w = \frac{z}{R} \qquad v = \frac{\rho}{R} \qquad b = \frac{Z'}{Z} \qquad \varepsilon = -\frac{ER}{Z}$$
$$m = \frac{L}{(ZR)^{1/2}} \qquad f = \frac{FR^2}{Z} \qquad r = \frac{ZR}{L^2} \tag{4}$$

our energy equation takes the following form:

$$\varepsilon = \frac{1}{\left(w^2+v^2\right)^{1/2}} + \frac{b}{\left[(1-w)^2+v^2\right]^{1/2}} + fw - \frac{m^2}{2v^2} \tag{5}$$

We can seek equilibrium points by finding partial derivatives of ε by the scaled coordinates w and v and setting them equal to zero. This will give the following two equations:

$$f + \frac{b(1-w)}{\left[(1-w)^2+v^2\right]^{3/2}} = \frac{w}{\left(w^2+v^2\right)^{3/2}} \tag{6}$$

$$\frac{m^2}{v^4} = \frac{1}{\left(w^2+v^2\right)^{3/2}} + \frac{b}{\left[(1-w)^2+v^2\right]^{3/2}} \tag{7}$$

From the definitions of the scaled quantities (4), $m^2 = 1/r$ and $E = -(Z/R)\varepsilon$. Because $r = ZR/L^2$, $E = -(Z/L)^2(\varepsilon/r)$, where $r = 1/m^2$ can be obtained by solving (7) for m. Substituting m into the energy equation, we get the three master equations for this configuration.

$$\varepsilon_1 = p^2\left\{\frac{1}{\left(w^2+p\right)^{3/2}} + \frac{b}{\left[(1-w)^2+p\right]^{3/2}}\right\} \times \left\{\frac{w^2+(p/2)}{\left(w^2+p\right)^{3/2}} + b\frac{(1-w)^2+(p/2)}{\left[(1-w)^2+p\right]^{3/2}} + fw\right\} \tag{8}$$

$$r = \left(p^2\left\{\frac{1}{\left(w^2+p\right)^{3/2}} + \frac{b}{\left[(1-w)^2+p\right]^{3/2}}\right\}\right)^{-1} \tag{9}$$

$$f + \frac{b(1-w)}{\left[(1-w)^2+p\right]^{3/2}} = \frac{w}{\left(w^2+p\right)^{3/2}} \tag{10}$$

where $E = -(Z/L)^2\varepsilon_1$ and $p = v^2$. Thus, ε_1 is the "true" scaled energy, whose equation for E does not include R. The scaled energy ε_1 and internuclear distance r in (8) and (9) now explicitly depend only on the coordinates w and p (besides the constants b and f). Therefore, if we solve (10) for p and substitute it into (8) and (9), we will have the parametric solution $\varepsilon_1(r)$ with the parameter w.

Our focus is at crossings of energy terms of the *same symmetry*. In the quantum TCC problem, "terms of the same symmetry" means terms of the same magnetic quantum number m [8–11]. Therefore, in our classical TCC problem, we fixed the angular momentum projection L and study the behavior of the classical energy at L = constant ≥ 0 (the results for L and $-L$ are physically the same).

Equation (10) does not allow an exact analytical solution for p. Therefore, we will use an approximate analytical method.

Figure 1 shows a contour plot of (10) for a relatively weak field $f = 0.3$ at $b = 3$, with w on the horizontal axis and p on the vertical. The plot has two branches. The left branch spans from $w = 0$ to $w = w_1$. The right one actually has a small two-valued region between some $w = w_3$ and 1 ($w_3 < 1$). Indeed, at $w = 1$, there are two values of p: $p = 0$ and $f^{(-2/3)} - 1$. Thus, the two-valued region exists only for $f < 1$.

Fig. 1. Contour plot of (10) for a relatively weak field $f = FR^2/Z = 0.3$ at $b = Z'/Z = 3$.

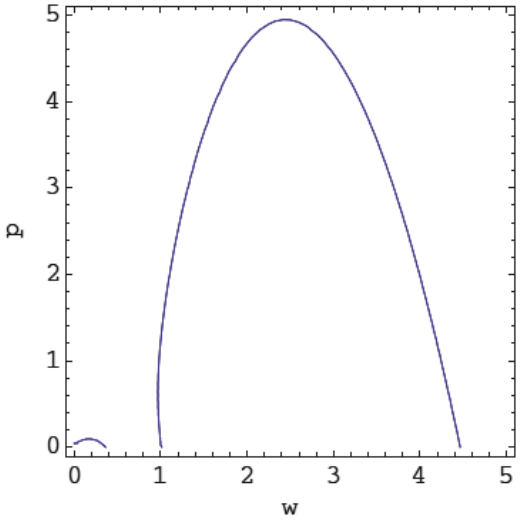

The right branch touches the abscissa at $w = 1$ and at some $w = w_2$. Analytical expressions for w_1 and w_2 are given in Appendix A. The quantity w_3 is a solution of the equation

$$f^{2/5}(2w_3 - 1)^{3/5} = w_3^{2/5} - b^{2/5}(1-w_3)^{2/5} \tag{11}$$

The method, by which w_3 was found from (11), is presented in Appendix B.

Figure 2 shows a contour plot of (10) for a relatively strong field $f = 20$ at $b = 3$. It is seen that there is no two-valued region.

Thus, Figs. 1 and 2 demonstrated the presence of the two branches and whether or not one of the branches has a two-valued region with respect to the scaled z-coordinate $w = z/R$. The contour plots facilitate obtaining further analytical results presented later.

From now on we consider the situation where the radius of the electronic orbit is relatively small, meaning that $p \ll 1$. Physically this corresponds to strong fields $f > f_{\min} \sim 10$.

Solving (10) in the small-p approximation, we obtain

$$p = \left\{w\left[f + \frac{b}{(1-w)^2}\right]^{-1}\right\}^{2/3} - w^2 \tag{12}$$

for the left branch ($0 < w < w_1$) and

$$p = \left[\frac{b(1-w)}{\left(1/w^2\right) - f}\right]^{2/3} - (1-w)^2 \tag{13}$$

for the right branch ($1 < w < w_2$). Substituting these results into (8) and (9), we get approximate solutions for energy terms $-\varepsilon_1(r)$ in both regions in a parametric form, w being the parameter. Now we plot classical energy terms $-\varepsilon_1(r)$ by varying the parameter w over both regions, using the appropriate formula for each one.

Fig. 2. Contour plot of (10) for a relatively strong field $f = FR^2/Z = 20$.

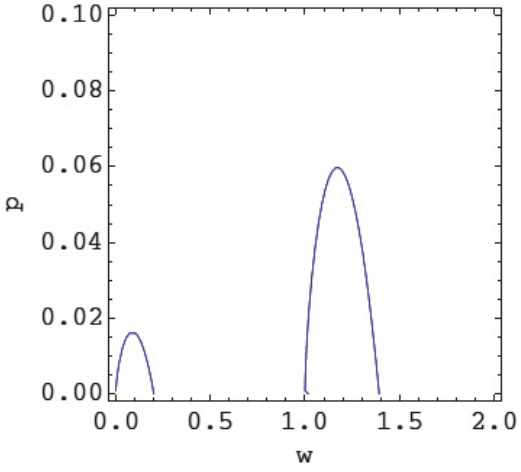

Fig. 3. Classical energy terms at $b = 3$ for $f = 100$.

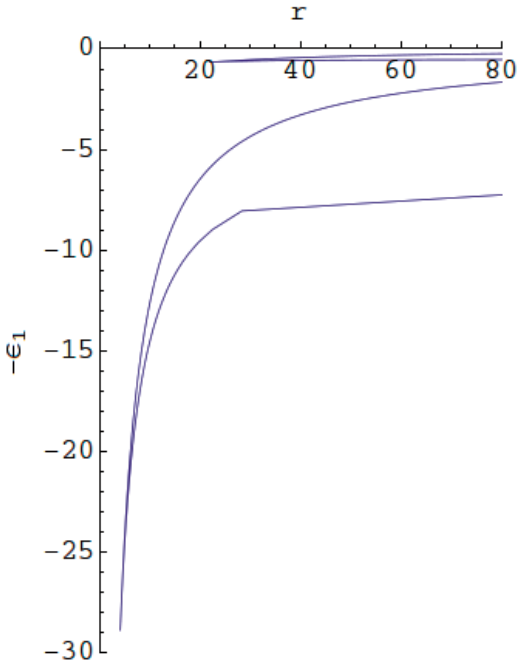

Figures 3, 4, and 5 show classical energy terms at $b = 3$ for $f = 100$, 20, and 5, respectively.

At this point it might be useful to clarify the relation between the classical energy terms $-\varepsilon_1(r)$ and the energy E. The former is a scaled quantity related to the energy as specified earlier in the first line after (10): $E = -(Z/L)^2\varepsilon_1$. The projection L of the angular momentum on the internuclear axis is a *continuous* variable. The energy E depends on both ε_1 and L. Therefore, while the scaled quantity ε_1 takes a *discrete* set of values, the energy E takes a *continuous* set of values (as it should be in classical physics).

We also solved the same problem numerically. By comparison we found that the approximate analytical solution is accurate for fields $f = 5$ and above.

Figures 6 and 7 show the numerically obtained classical energy terms at $b = 3$ for $f = 2$ and 0.1, respectively. For

Fig. 4. Classical energy terms at $b = 3$ for $f = 20$.

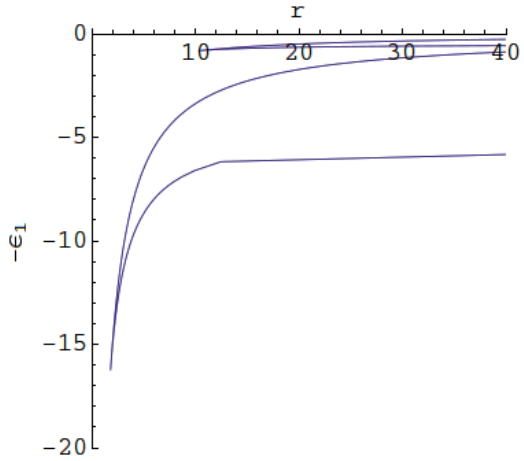

Fig. 5. Classical energy terms at $b = 3$ for $f = 5$.

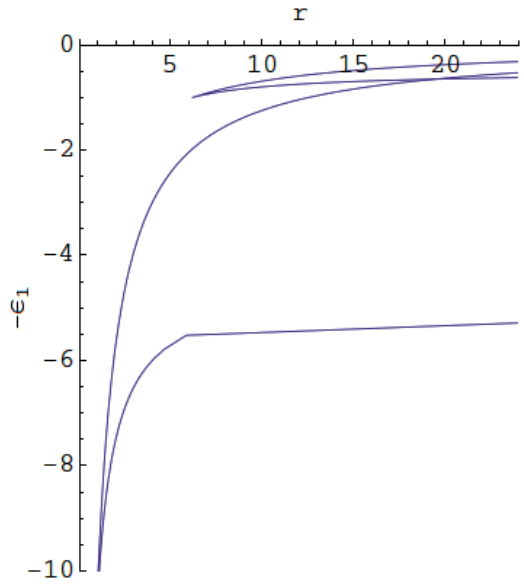

comparison, Fig. 8 shows the classical energy terms at $b = 3$ in the absence of the electric field (it had been previously presented by one of the authors in refs. 18 and 19).

The electric field causes several important new features compared to the zero-field case. While at $f = 0$ there are three classical energy terms, the electric field brings up the fourth classical energy term. Indeed, let us take as an example the case of $f = 5$ at $b = 3$ presented in Fig. 5. There are four energy terms that we label as follows:

1. the lowest term;
2. the next term up (which has a V-type crossing with term 1);
3. the next term up; and
4. the highest term (which has a V-type crossing with term 3).

We will use this labeling also while discussing all other plots (except the plot in Fig. 8 for $f = 0$): terms 1 and 2 will be those having a V-type crossing at lower energy, terms 3 and 4 will be those having a V-type crossing at higher energy,

Fig. 6. Classical energy terms at $b = 3$ for $f = 2$.

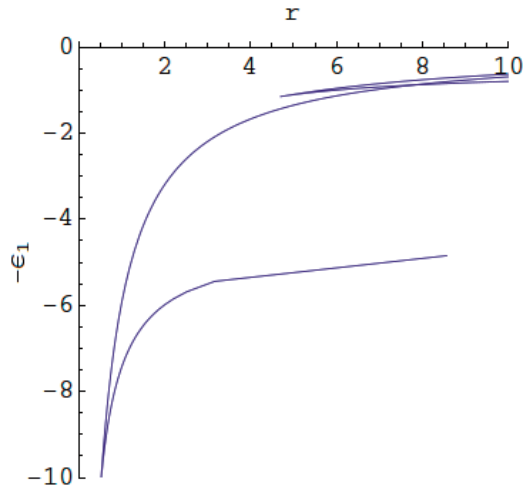

Fig. 7. Classical energy terms at $b = 3$ for $f = 0.1$.

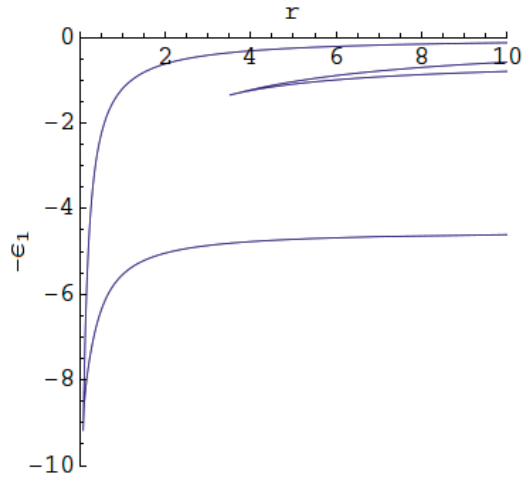

Fig. 8. Classical energy terms at $b = 3$ in the absence of the electric field.

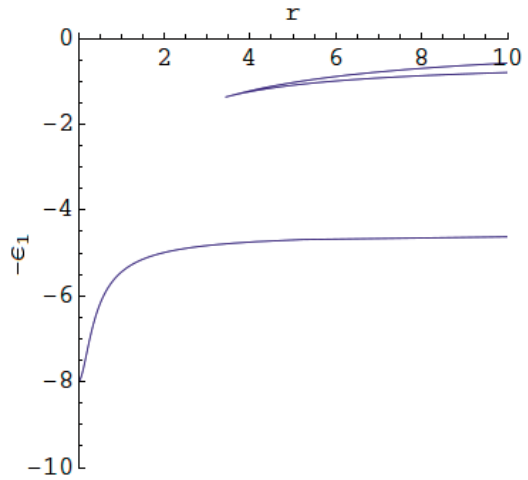

At $f = 0$ term 2 is absent, but it appears at any nonzero value of f no matter how small. Actually, as f approaches zero, this term behaves like $-f/r$, which is why it disappears at $f = 0$.

The existence of this additional term can be explained physically as follows. When $f = 0$, equilibrium of the orbital plane to the right of Z' (i. e., for $w > 1$) does not exist, so that the values of w_1 and w_3 reduce to the ones presented in refs. 18 and 19, and the right branch of $p(w)$ asymptotically goes to infinity when w goes down to w_3. When an infinitesimal field f appears, the right branch flips over positive infinity and ends up on the abscissa at $w_2 \to \infty$, thus enabling the whole region $w > 1$ for equilibrium. As the field grows, w_2 decreases. Physically, the force from the electric field at $w > 1$ balances out the Coulomb attraction of the Z–Z' system on the left — this situation is not possible for $f = 0$. This term is obtained by varying the parameter w from 1 to w_2.

We emphasize that the preceding example presented for $Z'/Z = 3$ represents a typical situation. In fact, *for any pair of* Z *and* $Z' \neq Z$, at the presence of the electric field, there are four classical energy terms of the same symmetry for CRS.

Another important new feature caused by the electric field is X-type crossings of the classical energy terms. These kinds of crossings and their physical consequences are discussed in the next section.

3. X-type crossings of classical energy terms and their physical consequences

Figure 9 shows a magnified version of the energy terms 2, 3, and 4 at $b = 3$ for $f = 2$. Figure 10 shows a further magnified version of the energy terms 2 and 4 at $b = 3$ for $f = 2$. Compared with Fig. 6 for the same b and f, in Figs. 9 and 10 we decreased the exhibited energy range, but increased the exhibited range of the internuclear distances r.

It is seen that term 2 has the X-type crossing with term 3 at $r = 7.8$ and the X-type crossing with term 4 at $r = 32$. The situation where there are two X-type crossings exists in a limited range of the electric fields. For example, for $b = 3$:

- two X-type crossings exist at $1.31 < f < 2.4$;
- there are no X-type crossings at $f < 1.31$; and
- there is one X-type crossing at $f > 2.4$ (the crossing of terms 2 and 3).

To reveal physical consequences of the X-type crossings, let us first discuss the origin of all four classical energy terms for arbitrary $Z'/Z \neq 1$. At $r \to \infty$, term 3 corresponds to the energy of a hydrogen-like ion of the nuclear charge $Z_{\min} = \min(Z', Z)$, slightly perturbed by the charge $Z_{\max} = \max(Z', Z)$, as shown in refs. 18 and 19.

At $r \to \infty$, term 4 corresponds to a near-zero energy state (where the electron is almost free), as shown in refs. 18 and 19. If the ratio Z'/Z is of the order of (but not equal to) unity, this term at $r \to \infty$ can be described only in the terminology of elliptical coordinates (rather than parabolic or spherical coordinates), meaning that even at $r \to \infty$ the electron is shared between the Z- and Z'-centers. However, in the case of $Z' \gg Z$, this term can be asymptotically considered as the Z'-term [18, 19]. It has the V-type crossing with term 3, which asymptotically is the Z-term ($Z_{\min} = Z$ for $Z' > Z$). Likewise, in the case of $Z' \ll Z$, term 4 can be asymptotically considered the Z-term [18, 19]. It has a V-type crossing with term 3, which asymptotically is the Z'-term ($Z_{\min} = Z'$ for $Z' < Z$).

Fig. 9. Magnified plot of the classical energy terms 2, 3, and 4 at $b = 3$ for $f = 2$.

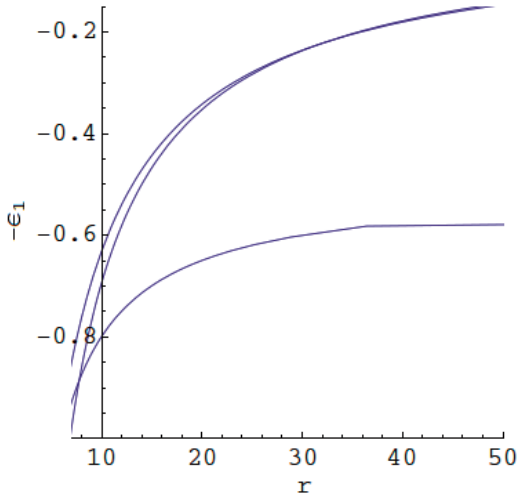

Fig. 10. Further magnified plot of the classical energy terms 2 and 4 at $b = 3$ for $f = 2$.

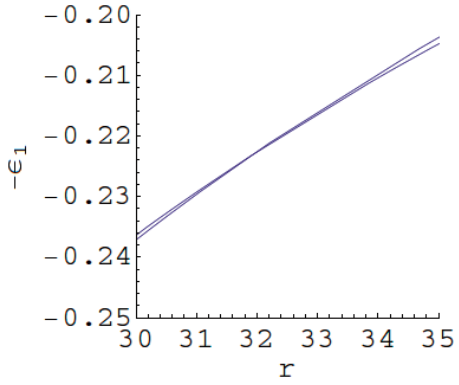

At $r \to \infty$, term 1 corresponds to the energy of a hydrogen-like ion of the nuclear charge Z_{max} slightly perturbed by the charge Z_{min} [18, 19]. As for term 2, at $r \to \infty$ it has properties similar to term 4, but with the interchange of Z_{max} and Z_{min}. In particular, in the case of $Z' \gg Z$, this term can be asymptotically considered as the Z-term, having the V-type crossing with term 1, which asymptotically is the Z'-term ($Z_{max} = Z'$ for $Z' > Z$). In the case of $Z' \ll Z$, term 2 can be asymptotically considered the Z'-term, having the V-type crossing with term 1, which asymptotically is the Z-term ($Z_{max} = Z$ for $Z' < Z$).

Thus, when Z and Z' differ significantly from each other, V-type crossings occur between two classical energy terms that can be asymptotically labeled as Z- and Z'-terms. This situation *classically depicts charge exchange*, as explained in refs. 18 and 19. Indeed, say, initially at $r \to \infty$, the electron was a part of the hydrogen-like ion of the nuclear charge Z_{min}. As the charges Z and Z' come relatively close to each other, the two terms undergo a V-type crossing and the electron is shared between the Z- and Z'-centers. Finally, as the charges Z and Z' go away from each other, the electron ends up as a part of the hydrogen-like ion of the nuclear charge Z_{max}.

So, the first distinction caused by the electric field is an additional, second V-type crossing leading to charge exchange — compared to the zero-field case where there was only one such crossing. However, the second V-type crossing (the crossing of terms 1 and 2) occurs at the internuclear distance $r_{V2} \ll r_{V1}$, where r_{V1} is the internuclear distance of the first V-type crossing (the crossing of terms 3 and 4). Therefore the cross section of the charge exchange corresponding to the second V-type crossing is much smaller than the corresponding cross section for the first V-type crossing.

Fig. 11. Dependence of the internuclear distance, where terms 3 and 4 cross, on the electric field at $b = 3$.

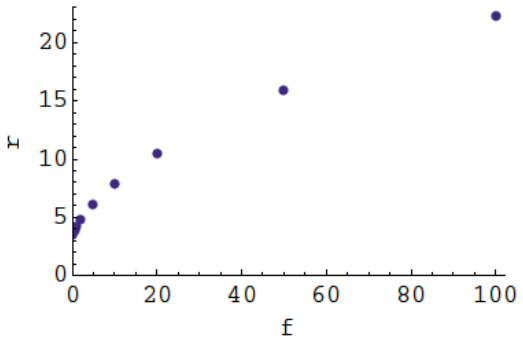

Fig. 12. Dependence of the internuclear distance, where terms 1 and 2 cross, on the electric field at $b = 3$.

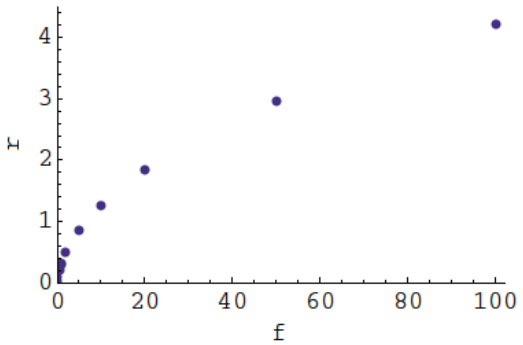

Figure 11 shows r_{V1} versus f and Fig. 12 shows r_{V2} versus f. It is seen that both quantities (and thus the cross sections of charge exchange) increase with the growth of the electric field.

Now let us discuss the X-type crossing from the same point of view. When Z and Z' differ significantly from each other, the X-type crossing of terms 2 and 4 is the crossing of terms that can be asymptotically labeled as Z- and Z'-terms. Thus, this situation again *classically depicts charge exchange*. The most important is that this crossing occurs at the internuclear distance $r_{X1} \gg r_{V1} \gg r_{V2}$. Therefore, the cross section of charge exchange due to this X-type crossing is much greater than the corresponding cross sections for the V-type crossings. This is the most fundamental physical consequence caused by the electric field: a *significant enhancement of charge exchange*.

When Z and Z' differ significantly from each other, the X-type crossing of terms 2 and 3 is the crossing of terms having the same asymptotic labeling: either both of them are Z-terms or both of them are Z'-terms. Therefore, this second X-type crossing (at $r = r_{X2}$) does not correspond to charge exchange, rather it represents an *additional ionization channel*. Indeed, say, initially at $r \to \infty$, the electron re-

sided on term 3 of the hydrogen-like ion of the nuclear charge Z. As the distance between the charges Z and Z' decreases to $r = r_{X2}$, the electron can switch to term 2, which asymptotically corresponds to a near-zero energy state (of the same hydrogen-like ion of the nuclear charge Z) where the electron would be almost free. So, as the charges Z and Z' go away from each other, the system undergoes ionization. Thus, another physical consequence caused by the electric field is the appearance of the additional ionization channel. This should have been expected as the electric field promotes the ionization of atomic and molecular systems.

4. Conclusion

We studied the effect of an electric field (along the internuclear axis) on CRS of the TCC system. We provided analytical results for strong fields, as well as numerical results for moderate fields. We showed that the electric field had the following effects.

The first effect is the appearance of an extra energy term — the fourth classical energy term — in addition to the three classical energy terms at zero field. This term exhibits a V-type crossing with the lowest energy term. The two highest energy terms continue having a V-type crossing, like at the zero field. In the situation where the charges Z' differ significantly from each other, both V-type crossings correspond to charge exchange.

The second effect is the appearance of a new type of crossing: X-type crossings. One of the X-type crossings (existing in a limited range of the electric field strength) corresponds to charge exchange at a much larger internuclear distance than the V-type crossings.

Therefore the cross section of charge exchange due to this X-type crossing is much greater than the cross section of charge exchange due to V-type crossings. Thus, the electric field can *significantly enhance charge exchange*. We believe that this is the most important result of the present paper.

The other X-type crossing does not correspond to charge exchange. Instead, it represents an *additional ionization channel*.

For completeness we add the following note concerning the corresponding quantum problem. The quantal energy terms are characterized by the elliptic quantum numbers k, s, m. Charge exchange can occur in the situation where two terms of the same symmetry ($m = m'$) differ by their "angular" elliptic quantum numbers $s = s' + 1$, while having the same "radial" quantum numbers $k = k'$. This situation corresponds to a quasi crossing (i.e., avoided crossing) of the two quantal terms.

One of the most important practical applications of our results is the following. Charge exchange in high temperature plasmas is strongly connected with problems of energy losses and of plasma diagnostics. Specifically, charge exchange between multicharged impurity ions and hydrogen (or deuterium, or tritium) atoms in tokamaks provides a nonlinear coupling of kinetics of impurities and neutrals, thus affecting the feasibility of controlled fusion (as multicharged ions produce considerably more radiative losses per unit particle than singly charged ions of the nuclear fuel components). A quasistatic electric field caused by plasma ions (the ion microfield) can strongly enhance charge exchange, as shown earlier, and thus affect the feasibility of controlled fusion significantly more than if the ion microfield was disregarded.

References

1. F.B. Rosmej and V.S. Lisitsa. Phys. Lett. A, **244**, 401 (1998). doi:10.1016/S0375-9601(98)00329-6.
2. R.C. Isler and R.E. Olson. Phys. Rev. A, **37**, 3399 (1988). doi:10.1103/PhysRevA.37.3399. PMID:9900083.
3. S.S. Churilov, L.A. Dorokhin, Yu.V. Sidelnikov, K.N. Koshelev, A. Schulz, and Yu.V. Ralchenko. Contrib. Plasma Phys. **40**, 167 (2000). doi:10.1002/(SICI)1521-3986(200004)40:1/2<167::AID-CTPP167>3.0.CO;2-W.
4. R.C. Elton. X-Ray lasers. Academic Press, New York. 1990.
5. F.I. Bunkin, V.I. Derzhiev, and S.I. Yakovlenko. Sov. J. Quantum Electron. **11**, 981 (1981). doi:10.1070/QE1981v011n08ABEH008162.
6. A.V. Vinogradov and I.I. Sobelman. Sov. Phys. JETP, **36**, 1115 (1973).
7. J. Von Neumann and E. Wigner. Phys. Z. **30**, 467 (1929).
8. S.S. Gershtein and V.D. Krivchenkov. Sov. Phys. JETP, **13**, 1044 (1961).
9. L.I. Ponomarev and T.P. Puzynina. Sov. Phys. JETP, **25**, 846 (1967).
10. J.D. Power. Philos. Trans. R. Soc. Lond. A, **274**, 663 (1973). doi:10.1098/rsta.1973.0079.
11. I.V. Komarov, L.I. Ponomarev, and S.Yu. Slavyanov. Spheroidal and Coulomb spheroidal functions. Nauka, Moscow. 1976. [in Russian].
12. St. Böddeker, H.-J. Kunze, and E. Oks. Phys. Rev. Lett. **75**, 4740 (1995). doi:10.1103/PhysRevLett.75.4740. PMID:10059985.
13. E. Oks and E. Leboucher-Dalimier. Phys. Rev. E, **62**, R3067 (2000). doi:10.1103/PhysRevE.62.R3067.
14. E. Oks and E. Leboucher-Dalimier. J. Phys. B, **33**, 3795 (2000). doi:10.1088/0953-4075/33/18/326.
15. E. Leboucher-Dalimier, E. Oks, E. Dufour, P. Sauvan, P. Angelo, R. Schott, and A. Poquerusse. Phys. Rev. E, **64**, 065401 (2001). doi:10.1103/PhysRevE.64.065401.
16. E. Leboucher-Dalimier, E. Oks, E. Dufour, P. Angelo, P. Sauvan, R. Schott, and A. Poquerusse. Eur. Phys. J. D, **20**, 269 (2002). doi:10.1140/epjd/e2002-00125-0.
17. E. Dalimier, E. Oks, O. Renner, and R. Schott. J. Phys. B, **40**, 909 (2007). doi:10.1088/0953-4075/40/5/007.
18. E. Oks. Phys. Rev. Lett. **85**, 2084 (2000). doi:10.1103/PhysRevLett.85.2084. PMID:10970468.
19. E. Oks. J. Phys. At. Mol. Opt. Phys. **33**, 3319 (2000). doi:10.1088/0953-4075/33/17/312.
20. M.R. Flannery and E. Oks. Phys. Rev. A, **73**, 013405 (2006). doi:10.1103/PhysRevA.73.013405.
21. E. Oks. Phys. Rev. E, **63**, 057401 (2001). doi:10.1103/PhysRevE.63.057401.
22. E. Lee, D. Farrelly, and T. Uzer. Opt. Express, **1**, 221 (1997). doi:10.1364/OE.1.000221. PMID:19373405.
23. T.C. Germann, D.R. Herschbach, M. Dunn, and D.K. Watson. Phys. Rev. Lett. **74**, 658 (1995). doi:10.1103/PhysRevLett.74.658. PMID:10058815.
24. C.H. Cheng, C.Y. Lee, and T.F. Gallagher. Phys. Rev. Lett. **73**, 3078 (1994). doi:10.1103/PhysRevLett.73.3078. PMID:10057282.
25. L. Chen, M. Cheret, F. Roussel, and G. Spiess. J. Phys. B, **26**, L437 (1993). doi:10.1088/0953-4075/26/15/002.
26. S.K. Dutta, D. Feldbaum, A. Walz-Flannigan, J.R. Guest, and

G. Raithel. Phys. Rev. Lett. **86**, 3993 (2001). doi:10.1103/PhysRevLett.86.3993. PMID:11328078.
27. R.G. Hulet, E.S. Hilfer, and D. Kleppner. Phys. Rev. Lett. **55**, 2137 (1985). doi:10.1103/PhysRevLett.55.2137. PMID: 10032058.
28. V.M. Vainberg, V.S. Popov, and A.V. Sergeev. Sov. Phys. JETP, **71**, 470 (1990).

Appendix A. The limits w_1 and w_2 on the graph of $p(w)$ in (10)

The analytical results for the quantities w_1 and w_2, obtained using the software Mathematica, have the following forms.

The expression for w_1 is

$$w_1 = \frac{\sqrt{3}}{6}\left(\sqrt{3} - \sqrt{\frac{(b+f-1)^2}{a_1 f} + \frac{a_1}{f} - \frac{2(b+f-1)}{f} + 3} + \sqrt{6\sqrt{3}(b+1)\left[f\sqrt{\frac{(b+f-1)^2}{a_1 f} + \frac{a_1}{f} - \frac{2(b+f-1)}{f} + 3}\right]^{-1} - \frac{(b+f-1)^2}{a_1 f} - \frac{a_1}{f} - \frac{4(b+f-1)}{f} + 6}\right)$$

where

$$a_1 = \sqrt[3]{54bf + (b+f-1)^3 + 6\sqrt{3bf}\sqrt{b^3 + 3b^2(f-1) + (f-1)^3 + 3b[1+f(f+7)]}}$$

The expression for w_2 is

$$w_2 = \frac{\sqrt{3}}{6}\left(\sqrt{3} + \sqrt{\frac{(b-f+1)^2}{a_2 f} + \frac{a_2}{f} + \frac{2(b+1)}{f} + 1} + \sqrt{6\sqrt{3}(b-1)\left[f\sqrt{\frac{(b-f+1)^2}{a_2 f} + \frac{a_2}{f} + \frac{2(b+1)}{f} + 1}\right]^{-1} - \frac{(b-f+1)^2}{a_2 f} - \frac{a_2}{f} + \frac{4(b+1)}{f} + 2}\right)$$

where

$$a_2 = \sqrt[3]{(f-1)^3 + 3b^2\Big(f-1) - b^3 - 3b[1+f(f+16)] + 6\sqrt{3bf}\sqrt{(b+1)^3 - 3f[1+b(b-7)] + 3f^2(b+1) - f^3}}$$

Appendix B. Finding the lower limit w_3 of the two-valued region on the graph of $p(w)$ in (10)

Defining a function

$$F(p,w) = f + \frac{b(1-w)}{\left[(1-w)^2 + p\right]^{3/2}} - \frac{w}{\left(w^2+p\right)^{3/2}} \tag{B1}$$

we can rewrite (10) as $F(p, w) = 0$. From the graph it is seen that at w_3, $\mathrm{d}w/\mathrm{d}p = 0$. Because $F(p, w) = 0$, $\mathrm{d}F/\mathrm{d}p = 0$ as well. On the other hand, $F(w, p) = F(w(p), p) = 0$ and

$$\frac{\mathrm{d}F}{\mathrm{d}p} = \frac{\partial F}{\partial w}\frac{\mathrm{d}w}{\mathrm{d}p} + \frac{\partial F}{\partial p} = 0 \tag{B2}$$

from which we get

$$\frac{\mathrm{d}w}{\mathrm{d}p} = -\frac{\partial F/\partial p}{\partial F/\partial w} \tag{B3}$$

Setting the right-hand side of (B1) and (B3) to zero, we obtain the system of two equations, solving which for w will give us the point on the contour plot of $F(p, w) = 0$ where the derivative $\mathrm{d}w/\mathrm{d}p$ vanishes (i.e., the desired point). Excluding p from the system, we reduce the equation to

$$f^{2/5}(2w_3 - 1)^{3/5} = w_3^{2/5} - b^{2/5}(1-w_3)^{2/5} \tag{B4}$$

where w was renamed to w_3 for clarity. This is (11) of the main text.